ELSEVIER

International Journal of Mass Spectrometry 223–224 (2003) 669–678

International Journal of Mass Spectrometry
www.elsevier.com/locate/ijms

# Radiative lifetime of vibrationally excited $N_2H^+$ and $N_2D^+$ molecular ions

M. Heninger[a], D. Lauvergnat[a], J. Lemaire[a], P. Boissel[a], G. Mauclaire[a,*], R. Marx[b]

[a] *Laboratoire de Chimie Physique (UMR 8000, associated to CNRS), Université Paris-Sud, Bât. 350, 91405 Orsay Cedex, France*
[b] *Université Paris-Sud, Bât. 300, 91405 Orsay Cedex, France*

Received 18 February 2002; accepted 17 June 2002

## Abstract

Vibrationally excited $N_2H^+$ and $N_2D^+$ ions with internal energies of at least 1.3 eV have been produced by electron ionization of a mixture of $N_2$ and $H_2$ (or $D_2$). Their radiative overall lifetime has been determined using the monitor ion technique in a triple cell ICR spectrometer.

Theoretical calculation of the vibrational energy levels up to 2.3 eV and of the radiative lifetimes for the fundamental transition of the three normal modes of each isotopomer has been performed in order to help the qualitative analysis of the experimental results.

Excitation of $\nu_1$ stretching mode is quickly relaxed and is not observed in our experimental conditions. The measured overall lifetimes correspond mainly to excitation of $\nu_2$ bending mode. Excitation of the $\nu_3$ stretching above $v = 2$ for $N_2H^+$ and $v = 3$ for $N_2D^+$ seems to be negligible. (Int J Mass Spectrom 223–224 (2003) 669–678)

*Keywords:* Radiative lifetimes; $N_2H^+$; $N_2D^+$; FT-MS; Monitor ion technique

## 1. Introduction

Protonated nitrogen $N_2H^+$ is an interesting molecular ion both because it has been identified as one of the constituents of interstellar clouds and because it is sufficiently simple to allow high level theoretical calculations and spectroscopic investigations.

However, there is a lack of information concerning the radiative lifetimes of vibrationally excited ions except for the $v = 1$ level of the N–H stretching mode $\nu_1$.

Production of vibrationally excited $N_2H^+$, by ion molecule reactions following electron impact ionization of hydrogen and nitrogen, has been demonstrated by Lindinger and coworkers [1] in an experiment carried out in a selected ion drift tube (SIDT) at Innsbrück.

The ions $N_2{}^+$, $H_2{}^+$ and $H_3{}^+$ are converted into $N_2H^+$ by the following ion molecule reactions:

$$N_2{}^+ + H_2 \rightarrow N_2H^+ + H, \quad (2.37\,\text{eV}) \tag{1}$$

$$H_2{}^+ + N_2 \rightarrow N_2H^+ + H, \quad (2.24\,\text{eV}) \tag{2}$$

$$H_3{}^+ + N_2 \rightarrow N_2H^+ + H_2, \quad (0.52\,\text{eV}) \tag{3}$$

All these reactions are fast and exothermic and it has been shown [2,3] that most of the reaction exothermicity is deposited as internal energy of $N_2H^+$. This has

---

[*] Corresponding author. E-mail: michel.heninger@lcp.u-psud.fr, gerard.mauclaire@lcp.u-psud.fr

1387-3806/02/$ – see front matter © 2002 Elsevier Science B.V. All rights reserved.
*PII* S1387-3806(02)00938-7

been confirmed by Villinger et al. [1], who observed the reaction of Kr with $N_2H^+$:

$$N_2H^+ + Kr \rightarrow KrH^+ + N_2 \quad (4)$$

This reaction which would be endothermic with ground state $N_2H^+$, can be fast only with excited $N_2H^+$. Three different rate constants were observed for reaction (4). They were tentatively assigned to ions excited in the $N_2$–$H^+$ stretching mode: $v = 0$ for the very slow reaction, $v = 1$ for the slow reaction and $v \geq 2$ for the fast exothermic reactions. The populations of these states have been estimated at 15, 36, and 49%, respectively.

At this time we had just started to investigate radiative relaxation of vibrationally excited ions using the monitor ion technique in a triple cell ICR spectrometer. After some preliminary results on $NO^+$ [4] and $HCO^+$ [5], $N_2H^+$ ions seemed to be interesting to study considering its importance in the chemistry of interstellar clouds and its similarity with $HCO^+$. However, the first results turned out to be too scattered to be published. Obviously, a better detection sensitivity and lower background pressure were needed to obtain reliable results.

A few years later Tosi et al. [6] showed, in a low energy crossed beam experiment of $N_2{}^+$ with $H_2$ ($D_2$), that the hydrogen atom transfer only proceeds via excited vibronic curves that correlate with excited states of the products.

This renewed our interest in investigating the radiative relaxation of excited $N_2H^+$(D) but we had to wait for an improved version of our instrument.

Implementation of a Fourier transform detection increased dramatically the sensitivity and modification of the cells shape and of the pumping system lowered the background pressure by a factor of 10. This new instrument has been used to investigate the radiative properties of quite a number of vibrationally excited diatomics [7–9] but of only two triatomics, H(D)$CO^+$ [10,11], and $H_2(D_2)O^+$ [12].

Indeed interpretation of the experimental results is much more difficult for triatomics than for diatomics because of the rapidly increasing density of vibrational states and the scarcity of theoretical results. However, since our interest in $N_2H^+$ had been promoted by a publication of Lindinger and coworkers [1], we decided to reinvestigate this ion more carefully and to present the results in this special issue dedicated to his memory.

## 2. Previous results

Protonated nitrogen has been the subject of a number of theoretical calculations and of only a few spectroscopic studies. Experiments as well as theory concern mainly ion structure and vibrational frequencies determination. Infrared band intensities have been calculated by Botschwina [13] for the two stretching modes $\nu_1$ and $\nu_3$ of $N_2H^+$ and its different isotopomers. The only experimental determination has been performed by Keim et al. [14], using direct laser absorption in fast ion beam (DLASFIB) first described by Owrutsky et al. [15].

Detection of the IR light absorption signal is possible only for rather strong transitions and, as discussed by Keim et al. [14], it is by no way straightforward to deduce integrated band intensities from the absorption signal. This is why integrated band intensity could be determined only for the $v = 1 \rightarrow 0$ transition of the $\nu_1$ stretching modes of $N_2H^+$ and $HCO^+$. Theoretical [13] and experimental [14] values of the IR band intensity of $N_2H^+$ are in good agreement, corresponding to a radiative lifetime of around 1.1 ms.

## 3. Present experiments

### 3.1. Apparatus

Determination of radiative lifetimes using the monitor ion technique in a triple cell FT-ICR spectrometer has been described several times [16,17]. Therefore, we will only recall its principles and stress the specificities of the present experiments.

The triple cell FT-ICR spectrometer is made up of three cascaded cells separated by ion funnels to allow the ions to be drifted from cell to cell while maintaining a pressure differential of around 250 between the low pressure central cell and the two adjacent cells: the ion production cell on one side, the reaction cell on the other [17].

The $N_2H^+$ ions are produced in the first cell and then trapped in the central cell for variable relaxation times. The background pressure, mainly $H_2O$, in this cell is $5 \times 10^{-9}$ Torr so that collisional relaxation is negligible compared to radiative relaxation except for very long lifetimes.

The ions are then drifted into the third cell where they react with a monitor gas M at constant pressure ($5 \times 10^{-6}$ Torr) during a constant reaction time (10 ms). At the end of the reaction time all the product ions and the unreacted $N_2H^+$ are drifted back into the central cell for detection by FT-ICR. Finally, the cell is emptied by a quench pulse and the sequence repeated for signal averaging.

### 3.2. Production of vibrationally excited $N_2H^+$ ions

A mixture of $H_2$ and $N_2$ (25 and 75%, respectively) is introduced in the source at a total pressure of $1.4 \times 10^{-5}$ Torr. This mixture is ionized by a 50 eV electron beam during 0.4 ms. The ions are then stored in the central part of the source cell in order to allow production of $N_2H^+$ by ion molecule reactions.

The reaction time is a compromise between the need of a large amount of $N_2H^+$ ions and the necessity to minimize collisional deactivation. The $N_2H^+$ ions are then mass selected and drifted into the low pressure relaxation cell.

However, since the low mass ions cannot be ejected efficiently, some of the unreacted ${H_2}^+$ and ${H_3}^+$ enter also the reaction cell.

### 3.3. The monitor reactions

As for $HCO^+$ [10] the monitor reactions used in these studies are proton transfer reactions with different neutrals:

$$N_2H^+ + M \rightarrow MH^+ + H_2 \tag{5}$$

In order to monitor vibrationally excited ions, M has to have a proton affinity smaller than that of $N_2$. Unfortunately, the proton affinity of $N_2$ being small (5.118 eV) [18] there are few available monitors (much less than for $HCO^+$). Only three suitable monitors have been found, Kr, $O_2$ and Ar, with proton affinities of 4.40, 4.363, and 3.826 eV, respectively [18].

The corresponding endothermicities of the monitor reactions are 0.718, 0.755, and 1.292 eV for $N_2H^+$ ground state. The difference in endothermicities due to the zero-point energy being small, the same values have been used for $N_2D^+$.

The proton transfer is fast for vibrational levels of $N_2H^+$ ions having an internal energy higher than the monitor reaction endothermicity and the number of monitor ions produced is proportional to the number of $N_2H^+$ ions in vibrational states located above the reaction threshold.

## 4. Experimental results

### 4.1. Radiative lifetimes

Fig. 1a and b shows a decay curve obtained for $N_2H^+$ and $N_2D^+$ reacting with Kr as monitor. All the decay curves corresponding to the three monitors $O_2$, Kr and Ar reacting with $N_2H^+$ and $N_2D^+$ can be analyzed as a sum of two exponentials giving a fast and a slow decay in addition to a small constant background signal. The fast decay correspond to the radiative cooling of $N_2H(D)^+$. The slow decay is at least partly due to reaction of the monitor molecules with ions other than $N_2H(D)^+$ as observed when $N_2H(D)^+$ is ejected before entering the reaction cell. These reactant ions are probably the remaining ${H_2}^+$ and ${H_3}^+$ that could not be ejected from the source. Therefore, the observed slow decay is difficult to analyze and the contribution of slowly decaying excited $N_2H(D)^+$ is impossible to determine. Table 1 displays the experimental lifetimes.

### 4.2. Reactivity of $N_2H(D)^+$ ions with the monitor gas

To determine the reactivity of $N_2H(D)^+$ ions with the different monitors, the $N_2H(D)^+$ ions produced in the first cell are drifted directly to the reaction cell

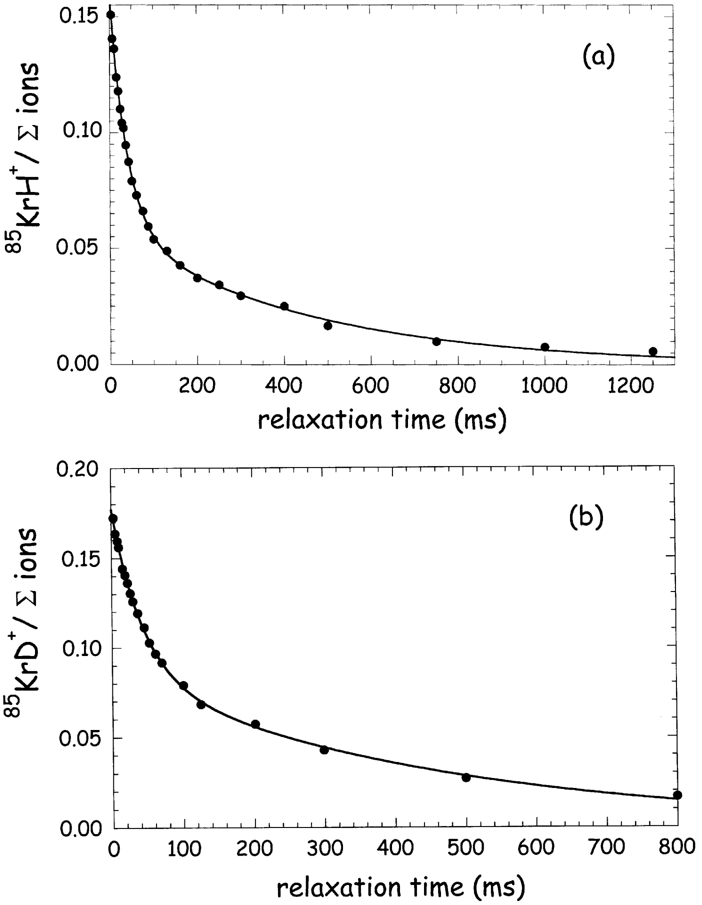

Fig. 1. Decay curves of the $KrH^+$ (a) and $KrD^+$ (b) monitor ions normalized to sum of the ions as a function of the relaxation time. Fitting a sum of two exponentials and a constant background signal to the experimental data gives: $\tau_s = 38.6$ ms, $\tau_l = 449$ ms for $N_2H^+$ and $\tau_s = 37.5$ ms, $\tau_l = 312$ ms for $N_2D^+$.

Table 1
Experimental decays (ms) have been obtained for each monitor by fitting the experimental curve to a sum of two exponentials and a constant background signal

| Monitor gas | $N_2H^+$ | $N_2D^+$ |
|---|---|---|
| Ar | 16 | 13 |
| | 164 | 224 |
| $O_2$ | 25.3 | 18 |
| | 450 | 326 |
| Kr | 38.6 | 37.5 |
| | 449 | 312 |

where they react with the monitor at constant pressure ($2 \times 10^{-6}$ Torr) and variable reaction time.

The time dependence of the relative intensities of the product ions for the reaction of $N_2H^+$ ions with Kr is reported in Fig. 2. The decay of $N_2H^+$ signal is fast at short reaction times and slow at long reaction times.

At short reaction times, vibrationally excited $N_2H^{+*}$ ions react with Kr to give $KrH^+$ ions. This reaction is in competition with the fast radiative relaxation (40 ms).

At longer reaction times the $N_2H^+$ ions are partly relaxed and their internal energy is too small to react

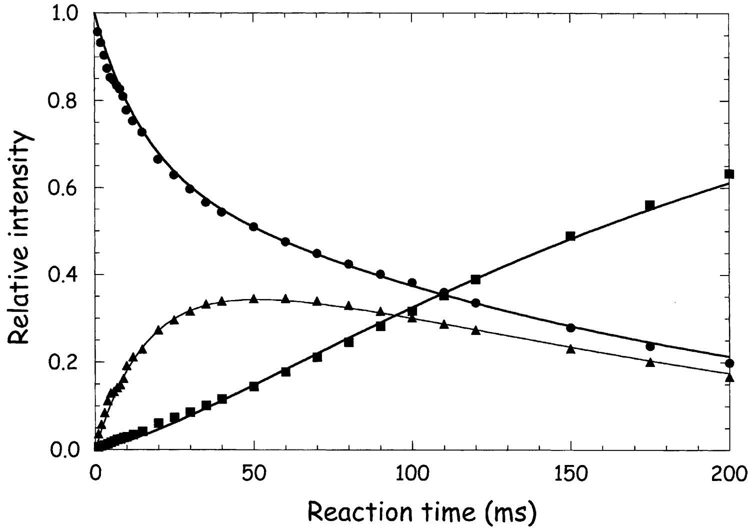

Fig. 2. Dependence of ions distribution with reaction time for the reaction of $N_2H^+$ with Kr: $N_2H^+$ (●), $H_3O^+$ (■), $KrH^+$ (▲). Lines are fits obtained with the KINET program (see text).

with Kr. However, Fig. 2 shows that the monitor ion $KrH^+$ is not the only product: at long reaction times $H_3O^+$ is also produced. This indicates that the slow decay of $N_2H^+$ is not only due to the monitor reaction but also to its reaction with residual $H_2O$ present in the reaction cell at a partial pressure of around $7 \times 10^{-8}$ Torr. Moreover, the monitor ion $KrH^+$ can also react with $H_2O$. These observations are summarized in the following scheme:

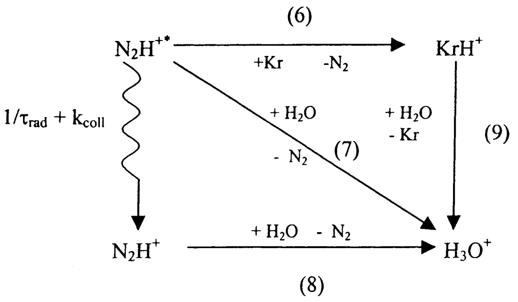

To check this reaction scheme and get the rate constants of the different processes, data analysis was performed using the KINET program [19].

The fraction of excited $N_2H^{+*}$ ions with at least 0.718 eV of internal energy is around 60%. The rate constants found for reactions (8) and (9) are fast ($2.3 \times 10^{-9}$ and $2.5 \times 10^{-9}$ $cm^3\,s^{-1}$) and very close to the calculated capture rate constants using the parametric formula of Su and Chesnavich [20] ($2.6 \times 10^{-9}$, $2.3 \times 10^{-9}$ $cm^3\,s^{-1}$). The rate constant of reaction (7) was not determined since it is a minor channel. The deactivation rate constant $1/\tau_{rad} + k_{coll}$ was found to be 0.0237 $ms^{-1}$ very close to the radiative relaxation rate 0.025 $ms^{-1}$ indicating that the collisional relaxation is negligible. The rate constant obtained for reaction (6) is $5.6 \times 10^{-10}$ $cm^3\,s^{-1}$ which is half of the capture rate constant $k_c = 1.15 \times 10^{-9}$ $cm^3\,s^{-1}$. Due to reaction of the remaining $H_2^+$ and $H_3^+$ on the monitor gas, it was not possible to analyze correctly the kinetics of the reaction of $N_2H^+$ with $O_2$ and argon.

## 5. Theoretical calculations

The aim of this theoretical section is to determine spectroscopic parameters (lifetime and spectrum) to help us with the qualitative analysis of our experimental results.

### 5.1. *Vibrational energy diagram*

The vibrational spectrum of both isotopomers has been calculated with a model, enabling the description of the isomerization process $(\mathrm{H{-}N_2})^+ \leftrightarrow (\mathrm{N_2{-}H})^+$. Indeed, the energy available in the reaction producing the ions is relatively high (up to 2.3 eV) thus, the bending amplitude motion may be large. Therefore, the set of Jacobi coordinates $\{\theta, r, R\}$ is well adapted to describe this process ($r$ is the distance between H and the center of mass G of $N_2$, $\theta$ the angle between (HG) and the bond axis of $N_2$, and $R$ is the N–N bond length). The vibrational energy diagram has been calculated using a model based on the harmonic adiabatic approximation (HADA) [21]. This method, explained in detail in [21], includes two main approximations:

(i) Instead of the available three-dimensional PES [22,23], we have used an expansion of the PES well adapted to the description of the isomerization process, namely a harmonic valley: along the minimum energy path in $\theta$, $V_0(\theta)$, only the quadratic expansion in $r$ and $R$ is kept. The determination of $V_0(\theta)$ has been performed at CCSD(T) [24–26] (coupled-cluster single, double and the perturbative contributions of connected triple excitations) level with the cc-pVQZ [27] basis set and using the optimized MP2/VTZ (Møller–Plesset perturbation theory to second order [28] level with the cc-pVTZ basis set [27]) geometry for 10 values of the Jacobi angle $\theta$ in the interval $[0^\circ, 90^\circ]$. The quadratic expansion in $r$ and $R$ is obtained with the help of the Hessian matrices calculated at the MP2/VTZ level. Finally, the analytical expressions of $V_0(\theta)$, the equilibrium parameters and the Hessian matrix elements have been fitted with the help of Legendre polynomials. All these calculations have been performed with the program MOLPRO2000.1 [29].

(ii) The wave function is expressed as a sum of products of a two-dimensional Harmonic-stretching wave function, $\psi_{(v_1,v_3)}(r, R; \theta)$, and one-dimensional bending function, $\varphi_k(\theta)$, developed on 40 even Legendre polynomials. The two-dimensional functions or the adiabatic states, $\psi_{(v_1,v_3)}$ are the eigenvectors of the Hamiltonian in $r$ and $R$ and define the adiabatic channels labeled with the two stretching quantum numbers $(v_1, v_3)$. Since the $\nu_1$ levels lifetimes (see Table 2) are too short to be observed in our experiments, only $n$ adiabatic channels in $v_3$ have been coupled (with $n = 9$ for $\mathrm{N_2{-}H^+}$ and $n = 10$ for $\mathrm{N_2{-}D^+}$).

Table 2
Lifetimes of the three normal modes of $N_2H^+$ and $N_2D^+$

| | | Experimental [14] (ms) | Theoretical [12] (ms) | Theoretical (MP2/VTZ) (present work) (ms) |
|---|---|---|---|---|
| $N_2H^+$ | $\nu_1$ | 1.1 | 1.1 | 1.1 |
| | $\nu_2$ | | | 123.1 |
| | $\nu_3$ | | 465.4 | 530.1 |
| $N_2D^+$ | $\nu_1$ | | 4.0 | 3.9 |
| | $\nu_2$ | | | 570.4 |
| | $\nu_3$ | | 28.1 | 45.7 |

Fig. 3a and b show the energy diagram of the vibrational levels of $N_2H^+$ and $N_2D^+$ for $v_1 = 0$. The model enables us to determine the weight of each adiabatic channel $(v_1 = 0, v_3)$ in a given vibrational state. The diagrams have then been split in six columns corresponding to the $v_3$ quantum number. In each column the length of the bar at a given energy stands for the percentage of the $v_3$ state in the decomposition. A 100% bar thus indicates a pure harmonic state, which occurs for $N_2H^+$ states below 1.5 eV. The harmonicity of the levels and the regularity of the $\nu_2$ levels progression, validates the use of the bi-harmonic model for the evaluation of the lifetimes of excited levels. The same conclusion can be derived in the case of $N_2D^+$ for energies lower than 1 eV, relevant for proton transfer with $O_2$ and Kr. It may be questionable at 1.29 eV where the mixing becomes much more important.

Due to the fact that the calculations are performed at total angular momentum $J = 0$, all the levels that would correspond to odd values of $v_2$ in a harmonic progression are absent. Therefore, to complete the diagrams on Fig. 3, one must add these levels half way between the even levels. This has been done in

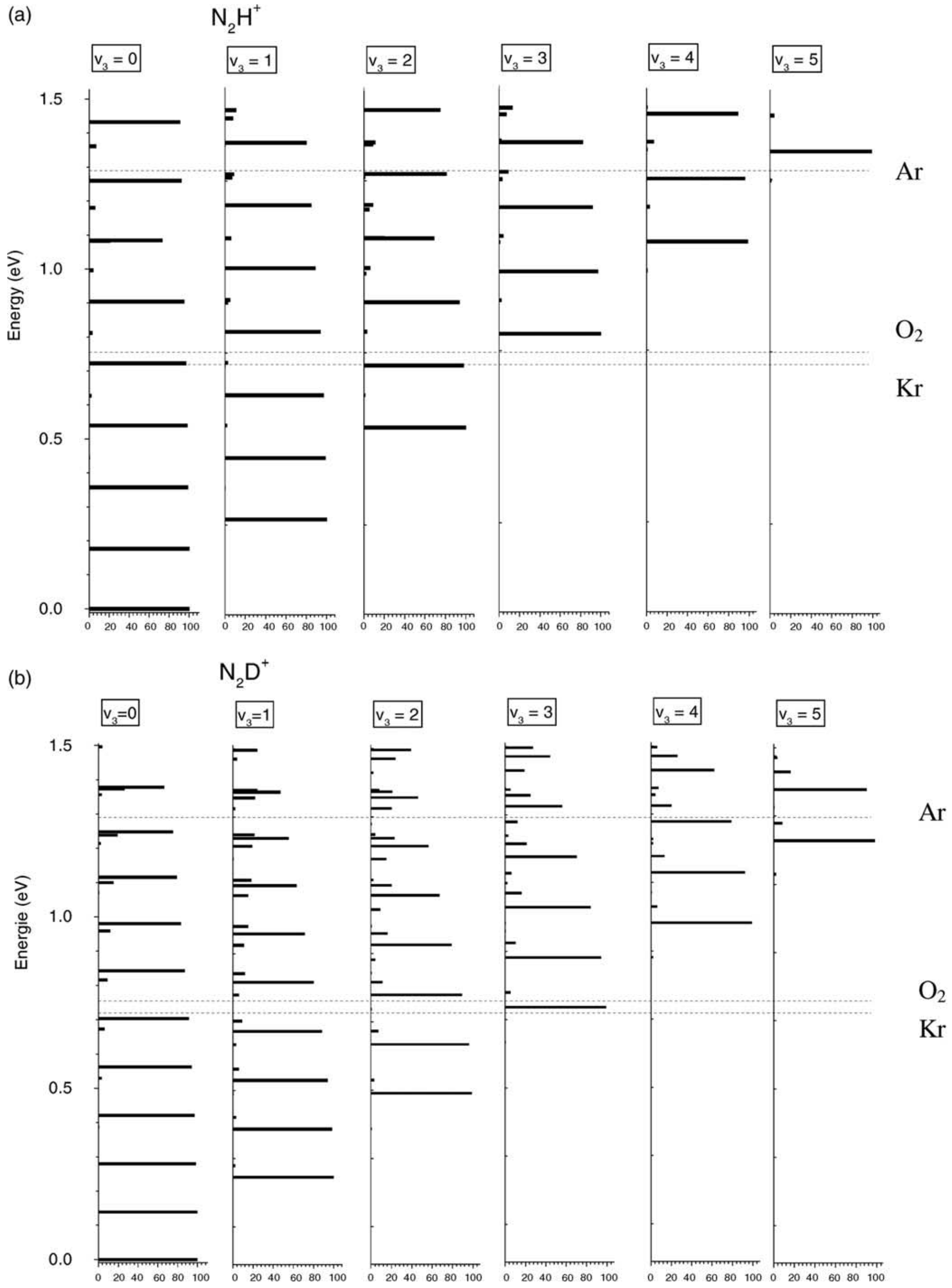

Fig. 3. Vibrational energy level diagrams of $N_2H^+$ (a) and $N_2D^+$ (b). Only levels with $v_1 = 0$ are represented. Each level is decomposed over the six adiabatic states $(v_1, v_3)$ with $v_1 = 0$ and $v_3 \in [0, 5]$. The length of the bars stands for the weight of each adiabatic state (see text). As the calculation is performed with $J = 0$ only even values of $v_2$ levels are represented. Dotted lines indicate the proton transfer threshold for the reactions with Kr (0.718 eV), $O_2$ (0.755 eV) and Ar (1.292 eV). This diagram does not include levels with $v_1 > 0$ which are expected to be quickly relaxed and levels with odd values of $v_2$ which does not come out of the calculation with $J = 0$.

Section 6 to determine the levels just above the proton transfer threshold. The agreement between calculated and experimental frequencies is quite satisfactory especially for the $\nu_2$ mode: 690 cm$^{-1}$ compared to 687 cm$^{-1}$ and 544 cm$^{-1}$ compared to 543 cm$^{-1}$ for $N_2H^+$ and $N_2D^+$, respectively.

### 5.2. *Lifetimes*

The intensities of the three fundamental transitions have been computed using the harmonic approximation at MP2/VTZ level with the help of GAUSSIAN 98 [30]. The corresponding lifetimes are in relatively good agreement with Botschwina's calculations [13] except for $\nu_3$ of $N_2D^+$ (see Table 2). The surprisingly large $\nu_3$ lifetime (or the small IR intensity) of $N_2H^+$, compared to that of the deuterated isotopomer has been explained by Botschwina [13]. In normal mode analysis, the lifetime is proportional to the inverse of $(\partial\mu/\partial Q_3)^2$ where $Q_3$ is the normal mode associated with $\nu_3$ harmonic frequency and $\mu$ is the dipole moment. Since the frequencies of the normal modes are rather different for the two isotopomers and the $Q_3$ component of the gradient of $\mu$ is much smaller for $N_2H^+$ than for $N_2D^+$, the $\nu_3$ lifetime of $N_2H^+$ is much longer than that of $N_2D^+$.

The present calculation gives the first complete set of radiative lifetimes for the three fundamental transitions of both $N_2H^+$ and $N_2D^+$. The excited states lifetimes can then be evaluated as explained below (see Section 6) and compared to the experimental lifetimes.

## 6. Identification of the measured lifetimes

The lifetime of $N_2H^+$ excited with one quantum in the $\nu_1$ stretching is well established ($\tau_1 = 1.1$ ms) experimentally and theoretically [13,14] and the lifetimes of levels with more than one quantum will be shorter. Therefore, the levels excited in the $\nu_1$ mode are quickly relaxed and cannot be observed, since the shortest relaxation time accessible in our experimental conditions, limited by the transit time of the $N_2H^+$ ions between the source and the reaction cell, is 2 ms. Then only the levels excited in the $\nu_2$ and $\nu_3$ modes can contribute to the observed lifetimes.

Since the initial distribution of the population among vibrational states is not known, the time evolution of the population of excited states probed by the monitor reactions cannot be calculated. In order to compare experimental and calculated results, we have assumed that the time evolution of the fraction of ions that can undergo the monitor reaction is governed by the population in the levels just above the threshold for the different reactions. These levels (see Fig. 3) are reported in Table 3 together with their

Table 3
Lifetimes of the levels probed by the different monitor gases for $N_2H^+$ and $N_2D^+$

| Monitor gas | Calculated | | | | | | | Experimental |
|---|---|---|---|---|---|---|---|---|
| $N_2H^+$ | | | | | | | | |
| Kr | Level | $8\nu_2$ | $\nu_3 + 5\nu_2$ | $2\nu_3 + 2\nu_2$ | $3\nu_3$ | | | |
| | $\tau$ | 15.3 | 23.5 | 49.9 | 176 | | | 38.6 |
| $O_2$ | Level | $9\nu_2$ | $\nu_3 + 6\nu_2$ | $2\nu_3 + 3\nu_2$ | $3\nu_3$ | | | |
| | $\tau$ | 13.7 | 19.8 | 35.5 | 176 | | | 25.3 |
| Ar | Level | $15\nu_2$ | $\nu_3 + 12\nu_2$ | $2\nu_3 + 9\nu_2$ | $4\nu_3 + 3\nu_2$ | $5\nu_3$ | | |
| | $\tau$ | 8.2 | 10 | 13 | 31.3 | 106 | | 16 |
| $N_2D^+$ | | | | | | | | |
| Kr | Level | $11\nu_2$ | $\nu_3 + 7\nu_2$ | $2\nu_3 + 4\nu_2$ | $3\nu_3$ | | | |
| | $\tau$ | 51.9 | 29.3 | 19.7 | 15.2 | | | 37.5 |
| $O_2$ | Level | $11\nu_2$ | $\nu_3 + 8\nu_2$ | $2\nu_3 + 4\nu_2$ | $3\nu_3+\nu_2$ | | | |
| | $\tau$ | 51.9 | 30.9 | 19.7 | 14.8 | | | 18 |
| Ar | Level | $19\nu_2$ | $\nu_3 + 15\nu_2$ | $2\nu_3 + 12\nu_2$ | $3\nu_3 + 8\nu_2$ | $4\nu_3 + 5\nu_2$ | $5\nu_3 + \nu_2$ | |
| | $\tau$ | 30 | 20.8 | 15.4 | 12.5 | 10.3 | 9 | 13 |

corresponding radiative lifetimes. In the double harmonic approximation, each level is characterized by quantum numbers $(0, v_2, v_3)$ with $v_2$ quanta in mode $\nu_2$ and $v_3$ quanta in mode $\nu_3$. Their lifetimes can then be estimated from the formula: $\tau_{ij} = 1/(v_2/\tau_2 + v_3/\tau_3)$ where $\tau_2$ and $\tau_3$ are the lifetimes of levels $(0, 1, 0)$ and $(0, 0, 1)$ given in Table 2.

For $N_2H^+$ two sets of lifetime values are found: $\tau < 50$ ms and $\tau > 100$ ms. The long lifetimes correspond to the part of the experimental decay curves that could not be analyzed (see Section 4.1). For each monitors an average of the calculated short lifetimes is in good agreement with the experimental value and the variation of the lifetimes with the monitor reaction is also correctly reproduced.

For $N_2D^+$, all the lifetimes are shorter than 53 ms and for each monitor the average of the calculated lifetimes is also in reasonable agreement with the experimental value. However, the rather large difference between the experimental lifetimes obtained with Kr and $O_2$ as monitors is somewhat surprising since their proton affinity differs only by the energy of one quantum of $\nu_2$. It looks like the efficiency of the different vibrational modes of $N_2D^+$ is not the same in the reaction of $O_2$ and Kr.

## 7. Conclusions

Vibrationally excited $N_2H^+$ and $N_2D^+$ ions have been produced by electron ionization of a mixture of $N_2$ and $H_2$ (or $D_2$). Proton transfer of these ions with Kr, $O_2$ and Ar has been used to monitor their radiative relaxation. Reaction with Ar shows that their energy content is at least 1.3 eV.

Calculation of the radiative lifetimes of the three normal modes of both isotopomers has been performed for the first time. It turns out that the bending mode relaxation is much slower for $N_2D^+$ than for $N_2H^+$ (570 ms compared to 123 ms) meanwhile the N–N stretching relaxes much faster in $N_2D^+$ than in $N_2H^+$ (45.7 ms compared to 530.1 ms). Since in our experimental conditions vibrational states with lifetimes shorter than about 2 ms cannot be observed, the energy cannot be stored in the short lived (1.1 ms) stretching mode as proposed by Villinger et al. [1]. Comparison of the experimental overall lifetimes with the calculated lifetimes of the vibrational levels probed by the different monitor molecules indicates that the energy is mainly located in the $\nu_2$ mode.

The rate constants of the monitor reactions are very difficult to determine because of several competitive processes (radiative decay of excited $N_2H(D)^+$ and reaction with $H_2O$). Therefore, no information on the energy content of the reacting excited state could be obtained through rate constants measurements.

## Acknowledgements

The authors thank Dr. Pascal Pernot for his contribution to data analysis.

## References

[1] H. Villinger, J.H. Futrell, A. Saxer, R. Richter, W. Lindinger, J. Chem. Phys. 80 (1984) 2543.
[2] Z. Herman, J. Kerstetter, T. Rose, R. Wolfgang, Discuss. Faraday Soc. 44 (1967) 123.
[3] R.D. Smith, J.H. Futrell, J. Phys. Chem. 81 (1977) 195.
[4] M. Heninger, S. Fenistein, M. Durup-Ferguson, E.E. Ferguson, R. Marx, G. Mauclaire, Chem. Phys. Lett. 131 (1986) 439.
[5] M. Heninger, Paris-sud, 1988.
[6] P. Tosi, O. Dmitrijev, D. Bassi, J. Chem. Phys. 97 (1992) 3333.
[7] S. Jullien, J. Lemaire, S. Fenistein, M. Heninger, G. Mauclaire, R. Marx, G. Chambaud, P. Rosmus, J. Chem. Phys. 101 (1994) 265.
[8] J. Lemaire, F. Mouchère, M. Heninger, S. Fenistein, R. Marx, G. Mauclaire, Int. J. Mass Spectrom. Ion Process. 172 (1998) 129.
[9] R. Marx, G. Mauclaire, S. Fenistein, J. Lemaire, M. Heninger, Int. J. Mass Spectrom. Ion Process. 165/166 (1997) 97.
[10] G. Mauclaire, J. Lemaire, M. Heninger, S. Fenistein, D.C. Parent, R. Marx, Int. J. Mass Spectrom. Ion Process. 149/150 (1995) 487.
[11] M. Heninger, J. Lemaire, S. Fenistein, R. Marx, G. Mauclaire, Int. J. Mass Spectrom. Ion Process. 185/186/187 (1999) 131.
[12] M. Heninger, J. Lemaire, G. Mauclaire, S. Fenistein, S. Jullien, R. Marx, J. Chem. Phys. 101 (1994) 1923.
[13] P. Botschwina, Chem. Phys. Lett. 107 (1984) 535.
[14] E.R. Keim, M.L. Polak, J.C. Owrutsky, J.V. Coe, R.J. Saykally, J. Chem. Phys. 93 (1990) 3111.

[15] J.C. Owrutsky, E.R. Keim, J.V. Coe, R.J. Saykally, J. Phys. Chem. 93 (1989) 5960.

[16] G. Mauclaire, M. Heninger, S. Fenistein, J. Wronka, R. Marx, Int. J. Mass Spectrom. Ion Process. 80 (1987) 99.

[17] R. Marx, S. Fenistein, G. Mauclaire, J. Lemaire, M. Heninger, Int. J. Mass Spectrom. Ion Process. 132 (1994) 143.

[18] E.P. Hunter, S.G. Lias, J. Phys. Chem. Ref. Data 27 (1998) 413.

[19] S. Le Caër, M. Heninger, P. Pernot, H. Mestdagh, Phys. Chem. Chem. Phys. 4 (2002) 1855.

[20] T. Su, W.J. Chesnavich, J. Chem. Phys. 76 (1982) 5183.

[21] D. Lauvergnat, A. Nauts, Y. Justum, X. Chapuisat, J. Chem. Phys. 114 (2001) 6592.

[22] F.A. Gianturco, S. Kumar, F. Schneider, Chem. Phys. 211 (1996) 33.

[23] S. Mahapatra, R. Vetter, Ch. Zuhrt, H.T. Nguyen, T. Ritschel, L. Zülicke, Chem. Phys. Lett. 285 (1998) 41.

[24] J. Cizek, Adv. Chem. Phys. 14 (1969) 35.

[25] C. Hampel, K.A. Peterson, H.J. Werner, Chem. Phys. Lett. 190 (1992) 1.

[26] J.D. Watts, J. Gauss, R.J. Bartlett, J. Chem. Phys. 98 (1993) 8718.

[27] T.H. Dunning, J. Chem. Phys. 90 (1989) 1007.

[28] C. Møller, M.S. Plesset, Phys. Rev. 46 (1934) 618.

[29] MOLPRO, is a package of ab initio programs written by H.-J. Werner, P.J. Knowles with contributions from R.D. Amos, A. Bernhardsson, A. Berning, P. Celani, D.L. Cooper, M.J.O. Deegan, A.J. Dobbyn, F. Eckert, C. Hampel, G. Hetzer, T. Korona, R. Lindh, A.W. Lloyd, S.J. McNicholas, F.R. Manby, W. Meyer, M.E. Mura, A. Nicklass, P. Palmieri, R. Pitzer, G. Rauhut, M. Schütz, H. Stoll, A.J. Stone, R. Tarroni, T. Thorsteinsson.

[30] M.J. Frisch, G.W. Trucks, H.B. Schlegel, G.E. Scuseria, M.A. Robb, J.R. Cheeseman, V.G. Zakrzewski, J.A. Montgomery, R.E. Stratmann, J.C. Burant, S. Dapprich, J.M. Millam, A.D. Daniels, K.N. Kudin, M.C. Strain, O. Farkas, J. Tomasi, V. Barone, M. Cossi, R. Cammi, B. Mennucci, C. Pomelli, C. Adamo, S. Clifford, J. Ochterski, G.A. Petersson, P.Y. Ayala, Q. Cui, K. Morokuma, D.K. Malick, A.D. Rabuck, K. Raghavachari, J.B. Foresman, J. Cioslowski, J.V. Ortiz, B.B. Stefanov, G. Liu, A. Liashenko, P. Piskorz, I. Komaromi, R. Gomperts, R.L. Martin, D.J. Fox, T. Keith, M.A. Al-Laham, C.Y. Peng, A. Nanayakkara, C. Gonzales, M. Challacombe, P.M.W. Gill, B.G. Johnson, W. Chen, M.W. Wong, J.L. Andres, M. Head-Gordon, E.S. Replogle, J.A. Pople, GAUSSIAN 98 Gaussian, Inc., Pittsburgh, 1998.